Sādhanā (2024)49:146
https://doi.org/10.1007/s12046-024-02514-y

Analysis of UNS S31603 ferrous joint made by rotary friction welding

S SENTHIL MURUGAN[1,*], S GIRISANKAR[1], C DEVANATHAN[1] and SUBHASCHANDRA KATTIMANI[2]

[1]Department of Mechanical Engineering, Rajalakshmi Engineering College (Autonomous), Chennai 602105, India
[2]Department of Mechanical Engineering, National Institute of Technology Karnataka , Surathkal 575025, India
e-mail: gctsegan@gmail.com

MS received 27 October 2023; revised 15 February 2024; accepted 21 February 2024

Abstract. This study delves into the effects of employing low friction pressure and high axial penetration during the fabrication of friction-welded joints using UNS S31603 stainless steel. The experiments were conducted using a continuous-drive rotary friction welding machine. Crucially, the research showcases the feasibility of creating robust welds in the metal, surpassing the strength of the parent metal. The resulting weld interfaces were remarkably narrow and well-defined. The mechanical properties of the welded joints, including tensile strength, yield strength, microhardness, impact toughness, and bending/flexural strength, were meticulously evaluated following ASTM standards. The findings indicate that the welded joints exhibited impressive tensile strength, approximately 803 MPa, and withstood a peak load of 52.0 kN. Additionally, these joints demonstrated a maximum elongation of 15.3% and a yield strength of 714.0 MPa. When subjected to bending conditions, similar joints made of UNS S31603 withstood loads of up to 19.0 kN before experiencing crack propagation. Ductility was observed in the fracture mode within the weld region, characterized by the formation of cup and cone necking, highlighting the joints' ductile behaviour. Furthermore, the joint efficiency was calculated to be over 100%. Utilizing these specific parameters, this method resulted in a maximum axial shortening or material loss of approximately 14 mm.

Keywords. UNS S31603 steel; tensile strength; Vickers hardness; grains; austenite; friction welding.

1. Introduction

UNS S31603 (A4 stainless steel/AISI316L) alloy offers exceptional durability and corrosion resistance, surpassing traditional steel. Its widespread use in various industries, particularly in marine and food processing equipment applications, is inevitable due to these outstanding properties. A4 stainless steel is highly recommended in situations where higher temperatures could trigger corrosion. The fabrication of components for these industries involves advanced welding techniques. This versatile metal finds extensive applications, including the production of aero engine parts and engine-bladed disks [1]. A4 steel requires low heat for welding due to its low heat conductivity, preventing heat from dissipating quickly [2]. Fusion welding exhibits impressive results when used on A4 steel, both with or without filler material. However, it comes with limitations, including complexities, circular rod welding challenges, a large heat-affected zone, solidification cracking, and undesirable colour changes around the weld. Gas welding is not advisable for A4 steel. A superior alternative for joining A4 stainless steel rods is the frictional joining/friction welding (FW)/solid-state technique. This method, a solid-state joining process [3], does not melt the parent metal (PM) since its welding temperature requirement is lower than the base metal's melting point. FW is also suitable for joining dissimilar alloys. Unlike fusion welding of A4 steel, post-weld heat treatment is unnecessary in FW, although it might be required in traditional fusion welding methods. The typical FW setup is depicted in figures 1(a) and (b). In FW, two workpieces are rubbed together under pressure, generating heat. This localized heat leads to material melting and subsequent bonding. FW produces high-quality weld joints between similar or dissimilar metals by creating heat through mechanical friction. The workpieces, moving relative to each other, experience a lateral force known as an upset force, causing plastic displacement and fusion of the base materials at their contact surfaces. Ahmadi and Ebrahimi [4], conducted a study on TIG welding of AISI 316L alloy and observed that adding flux could enhance the percentage of delta-ferrite, consequently increasing the tensile strength of the weld. The KUKA FW machine used in this study is depicted in figure 1(c). Other studies, such as those by

*For correspondence
Published online: 17 April 2024

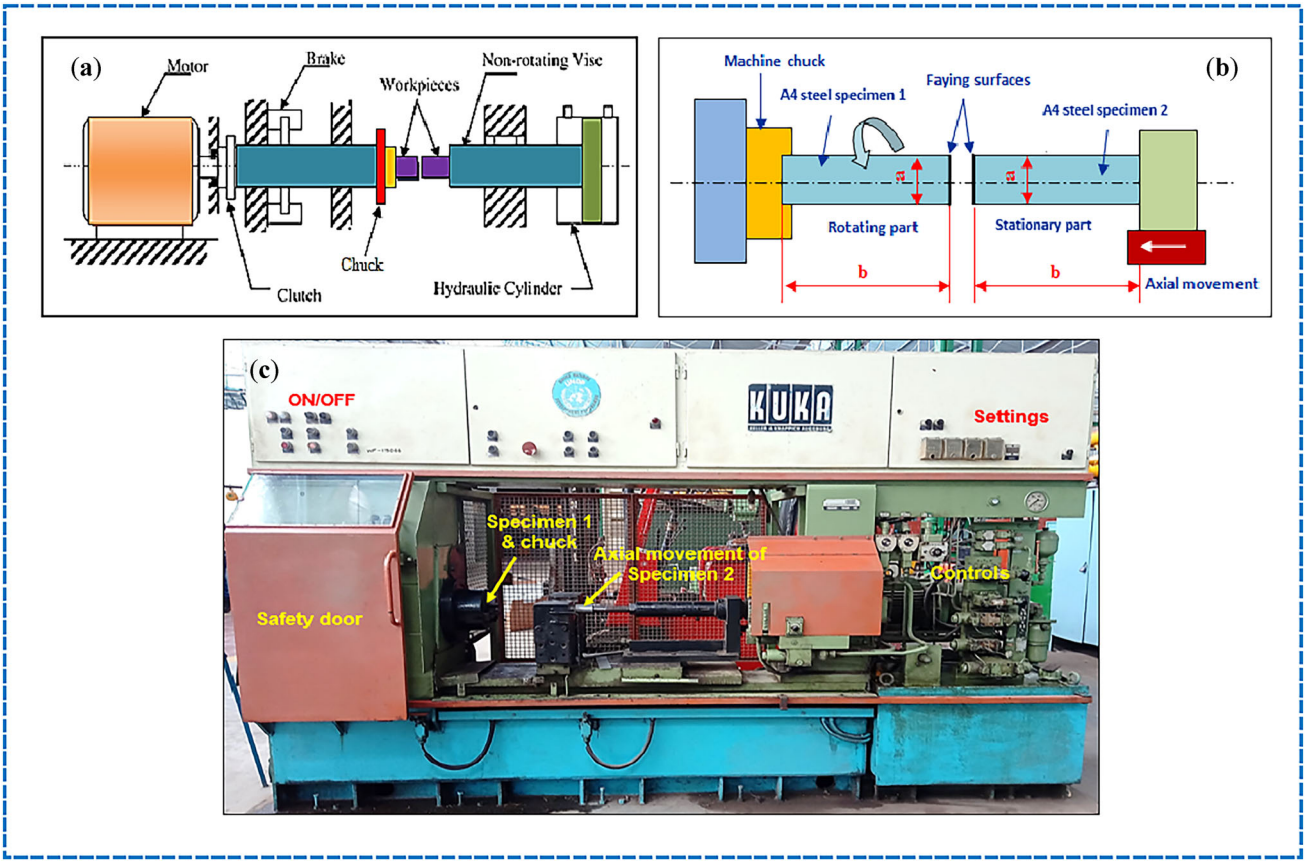

Figure 1. (**a**) Schematic diagram of friction welding set-up [5], (**b**) welding concept used in this study with a = ϕ12 mm, b = 100 mm specimens and (**c**) FW machine used.

Senthil *et al* [6–8], have demonstrated the potential of FW with various faying surface modifications, leading to improved properties. Incorporating techniques such as geometrical modifications and surface alterations in the faying surface, such as ceramic coating and electrodeposition, along with interlayer concepts between faying surfaces, can result in robust welds and enhance the performance of the FW method on samples. Wan and Huang [9], investigated FW of A4 steel with AA6061 alloy and noted that reducing friction time led to a decrease in the thickness of the IMC layer. The authors utilized a collar on the AA6061 side to control flash and weld expulsion. Meanwhile, Li *et al* [10] successfully joined 316L alloy with TC4 alloy, observing inhomogeneous interfaces along with a fully dynamic recrystallized zone featuring equiaxed grains. Khidhir and Baban [11] explored the fusion of 316L (A4 steel) with 1045 steel. The authors noted that increasing forging pressure raised hardness values, yet led to decreased tensile values, resulting in a maximum joint efficiency of 90.0%. Mishra Neeraj Kumar and Shrivastava Amber [12] noted the recrystallization (dynamic) and severe plastic deformation in the interface region especially in the 316L alloy side when the rotary FW of it with Inconel alloy in the presence of metal interlayer, which in turn increased the strength and ductility of the joint. Meanwhile, Cetkin *et al* [13] investigated frictional joining between Ramor and 316 steel, achieving a maximum of approximately 580 MPa. They demonstrated that parameters significantly influenced the properties and structure of the joints. Antonino Squillace *et al* [14] identified brittle intermetallic compounds forming cracks in the weld zone during dissimilar FW of 316L with a titanium alloy. Extensive research has been conducted on joining A4 stainless steel with various materials, yet limited attention has been given to joining A4 steel rods with themselves (similar joining). Specifically, continuous drive rotary friction welding (RFW) [15] with minimal pressures has been underexplored in this context. In research, Çavuşoğlu [16] observed that the tensile strength of the AISI 4140/IN713C dissimilar joint was positively influenced by an elevation in forging pressure and friction time. The morphology of the FW's joint may depend on the RFW's parameters [17]. The substantial deformation resulting from the high forging pressure led to an extended burn-off, whereas minor deformation stemming from low forging pressure resulted in a brief burn-off. Prolonged friction time has the potential to compromise the strength of the weld by fostering the formation of an oxide layer over the faying

surfaces throughout the extended thermal cycle. Oxidation during friction welding can occur despite the faying surfaces being pressed hard against each other and not directly exposed to the atmosphere. This phenomenon may happen due to the presence of residual oxygen and other oxidizing agents within the materials being welded, as well as the heat generated during the friction welding process. Ambient air can enter the welding zone during the process, allowing oxygen to react with the heated surfaces and promote oxidation. So, a perfect sealing or controlled environmental state is required to minimize oxidation and improve the quality of the weld.

Jignesh Patel *et al* [18] reported from the results of RFW of Invar-SS304 alloys that the higher friction pressure and increase in m/c spindle speed resulted in lower tensile strength due to non-homogeneous temperature distribution at the weld interface. An increase in friction pressure has the potential to widen the region of higher hardness, and the overall axial shortening of the joint rises in tandem with an increase in forging pressure. The research on joining AA6061/AISI316L stated that the increase in friction time increased the thickness of IMC layers [9]. This study aims to weld small-diameter A4 steel rods (similar welding) with flat surfaces utilizing rotary friction welding at low process parameters. The objective is to achieve a homogeneous weld interface and examine the correlated mechanical properties. This research is vital due to A4 steel's suitability for marine applications, including valves, pumps, propeller shafts, tubing, piping, marine structures, desalination equipment, boat fittings, sensors, sub-sea connectors, as well as handrails and guardrails on ships. Understanding the fundamentals of frictional joining in A4 steel is essential. This study endeavours to provide essential insights into the process, contributing to the knowledge base in materials engineering and facilitating advancements in marine technology.

2. Materials and methods

A4 austenitic stainless steel, also known as Alloy UNS S31603 or 1.4404, is a chromium-nickel-molybdenum steel renowned for its exceptional properties. This steel, detailed in table 1, boasts excellent corrosion resistance and is highly popular worldwide. The addition of Molybdenum enhances its corrosion resistance, making it ideal for marine applications. Additionally, it exhibits high oxidation resistance at elevated temperatures and resists intergranular corrosion in welded conditions. Notably, it retains impressive strength and hardness even at low temperatures, including cryogenic conditions. For specific material properties and applications, refer to table 2. In various industries, the necessity to weld hard materials is unavoidable. RFW stands out as a crucial technique for joining circular rods made of similar or dissimilar alloys due to its ability to create a narrow heat-affected zone (HAZ) and achieve efficient results in less time. In this study, two UNS S31603 rods (each 108 mm in length and 12 mm in diameter) were successfully joined using a rotary friction welding machine (Model: KUKA, Germany). The welding parameters employed included 2 MPa of friction pressure, 4 MPa of forging pressure, 4 seconds of friction time, 4 seconds of upset time, and an axial penetration of 6 mm/s, as detailed in table 3. A successful welding process for UNS S31603 alloy was achieved using low frictional pressure. Figure 2(a) displays the prepared specimens, while figures 2(b) and (d) showcase the resulting weldments. The flash-butt weldment, illustrated in figure 2(c), exhibited flash generation of approximately 5 mm on each side due to excessive friction, a consequence of the hardening effect experienced by UNS S31603 alloy during the joining process. The amount of flash formed depended on the material's nature and welding parameters such as penetration feed and welding speed. During the experiments, it was observed that there was no penetration of one side specimen into the other, and an equal amount of flash formation occurred on both sides while welding hard UNS S31603 alloy rods. This occurrence is common in similar welding processes. To assess their stability, the welded joints were subjected to a drop test from a height of 1 meter above the ground. Specimens prepared from the weldments, following ASTM standards, successfully underwent the drop test to evaluate their mechanical properties and microstructural characteristics.

Table 1. Elemental composition of UNS S31603 steel alloy [9].

C	Mn	Si	Cr	Ni	Mo	P	S	N	Fe
0.025	1.9	0.75	18.0	12.3	2.0	0.035	0.03	0.1	Bal.

3. Results and discussion

3.1 *Observation and structural study*

The welded similar joints were sectioned along its length using a wire-EDM machine and the images of the cross-sectioned welds are given in figures 2(e) and (f) (before polishing). The weldment prepared for structural characterization, as shown in figure 3(a) (after polishing), exhibits a distinctly curved flash formation, indicating successful welding where the parameters met the required standards. The formed flash demonstrated minimal material loss on the specimen and a thin weld interface (WI) without any signs of welding defects. This flawless welding example highlights that a frictional pressure of around 2 MPa is sufficient for butt-joining 12 mm diameter A4 steel alloy cylindrical rods. Figure 3(b) presents the macrostructure of the friction-welded A4 alloy butt joint, displaying a defect-free weld zone and parent material. The heat-affected zone

Table 2. Properties, advantages and applications of UNS S31603 steel alloy.

Property	Value	Advantages	Applications
(a) Density (g/cc)	8.03	Good corrosion resistance, good formability, high strength, good weldability	Chemical processing equipment, food processing equipment, marine applications, etc.
(b) Elongation (%)	40		
(c) Compressive stress (MPa) (min.)	170		
(d) Tensile strength (MPa) (min.)	485		
(e) Young modulus (GPa) (min.)	190		
(f) Yield strength (MPa) (min.)	195		

in the middle appears narrow, and the extracted material, observed as a spiral-shaped flash on both sides, illustrates the effective frictional contact between the faying surfaces of the A4 steel specimen. The etching was done on the surface of the samples by dipping for 20 seconds at room temperature with V2A etchant (a solution of 100 ml distilled water, 100 ml HCL, and 10 ml nitric acid) for taking microstructure. Optical micrograph images of the welded A4 steel joint's left and right sides (figures 4(a) and (b) reveal austenite structures, imparting excellent toughness to the weld). The grains near the weld interfaces appear refined due to the impact of friction pressure, emphasizing the crucial role played by friction pressure. The narrow weld interface, highlighted in image 4(c), lacks any visible scars, indicating the flawless bonding between the two weld specimens. In their study, Liu and Fujii [19] noted the presence of a thin and robust intermetallic layer at high friction pressure. Conversely, on the 316L alloy side during FW, a substantial faying surface deformation was observed. This research underscores the significance of friction welding, demonstrating impeccable bonding achieved during experimentation.

3.2 *Axial shortening*

Axial shortening refers to the material losses experienced by the weld specimen after the friction welding process. In simpler terms, it signifies the decrease in the length of the workpieces being joined as a consequence of the welding operation. This phenomenon occurs during friction welding due to the high heat generated at the interface of the workpieces. As the materials rub against each other and heat up, they soften and melt together. This fusion process leads to a reduction in the initial length of the workpieces. Figure 5 presents the values obtained from all the conducted trials. Initially, the total length of the weld specimen was 206 mm, and after the friction welding process, the corresponding weldment measured about 192.5 mm. It was observed that the material loss remained relatively consistent across all trials. Based on this observation, it can be deduced that a reduction of 13.54 mm in material length was achievable after the welding process. Ome Karabey and Ahmet Akkus [20] have noted that axial shortening varies with changes in friction pressure and friction time. The extent of axial shortening is influenced by multiple factors, encompassing material properties, welding parameters (such as rotational speed, pressure, and duration), as well as the geometrical dimensions and shape of the workpieces. Excessive reduction in length is not recommended in friction welding. To achieve precise and dependable friction welds while mitigating axial shortening, meticulous planning, rigorous process control, and thoughtful material selection are indispensable. It is crucial to note that the magnitude of axial shortening varies across different metals and alloys, contingent on their composition and specific process parameters.

3.3 *Tensile property and joint efficiency of prepared weld*

Tensile strength serves as a vital measure of weld quality, assessing its strength and reliability. To evaluate the welded specimen, an initial drop test from a height of one meter was conducted. If the specimen successfully passed this drop test, it proceeded to the tensile testing phase. The tensile testing specimen was meticulously prepared from the fabricated weld specimen following the guidelines outlined in standard ASTM E8, as depicted in figure 6(a). Notably, no signs of scars or defects were identified in the welding area. This demonstrates a flawlessly executed, clean welding process. The tensile test plays a pivotal role in determining crucial factors such as strength, ductility, joint efficiency, and elongation. When evaluating the tensile properties of friction-welded A4 stainless steel, several factors come into play, including the heat-affected zone (HAZ), welding parameters, and microstructure. Despite the material's inherent good strength, ductility, weldability, and corrosion resistance, the specific properties and microstructure can vary significantly based on the chosen weld parameters and the heat input. The tensile test results are illustrated in figures 6(b) to (e). The tensile fracture occurred within the gauge length of the tensile sample, near

Table 3. Experimental parameters for FW.

Trial no.	Friction pressure (bar)	Upsetting pressure (bar)	Heating time (sec.)	Upset time (sec.)	Spindle speed (rpm)	Feed rate (mm/sec)
1 to 5	20	40	4	4	1500	6

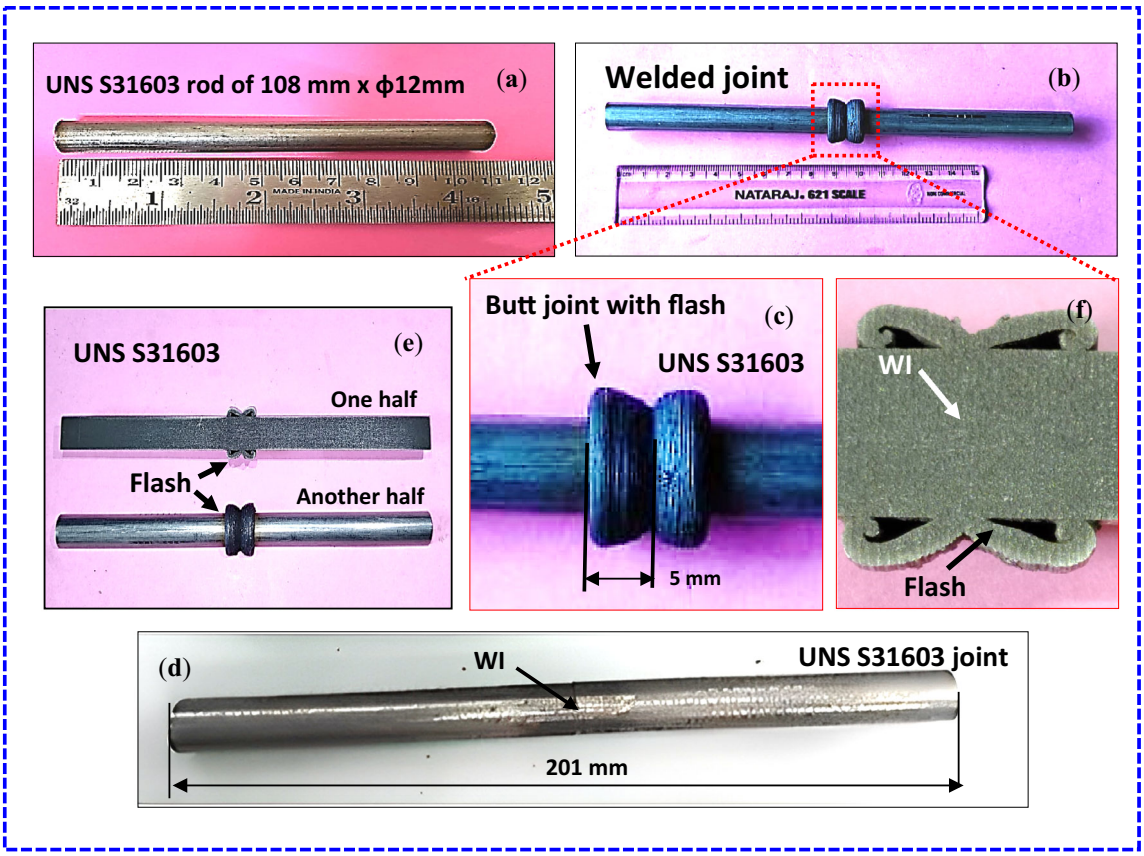

Figure 2. (**a**) specimen before facing and welding, (**b**) weldment after welding before machining, (**c**) flash-butt, (**d**) similar weld joint after machining, (**e**) two halves of the welded sample and (**f**) cross-section of the weld.

the weld zone, rather than directly within the weld itself. The experimentation unequivocally demonstrated that the welding process and its parameters exert a substantial influence on both the microstructure and the strength of the parent metal (PM). Notably, the tensile strength of the weld reached approximately 803 MPa as a maximum at a low welding pressure. This value significantly surpasses the strength of the A4 parent metal, which we determined to be approximately 545 MPa based on our testing of the PM sample. It is also notably higher than the supplier-recommended minimum value of 485 MPa (as indicated in table 2). During FW, material flow and mixing occur at the faying surfaces' interface, leading to the formation of a homogeneous welded joint. Thus it facilitates good bond formation. The welded sample endured the applied load until it reached a peak load of 52.5 kN during testing. Analyzing the load vs. deflection curve, it was evident that stress remained proportional to strain, obeying Hooke's law, up to 4 mm and ultimate yielding reached 4.5 mm. Beyond this point, a slight deviation occurred in the curve, leading to an increase in strain, while the stress gradually rose until it reached its maximum load at 7 mm. During the pulling process, the weld metal underwent some plastic deformation, and eventually, it fractured, causing the load to abruptly drop at 12 mm. Though the strength was good, it showed poor ductility as its elastic elongation is half of the total elongation. The microstructure of the welded joint, especially within the heat-affected zone, significantly influences its tensile properties. The rapid heating and cooling cycles during the friction welding process can result in varied microstructures, impacting the mechanical properties. The refined microstructure enhances the tensile

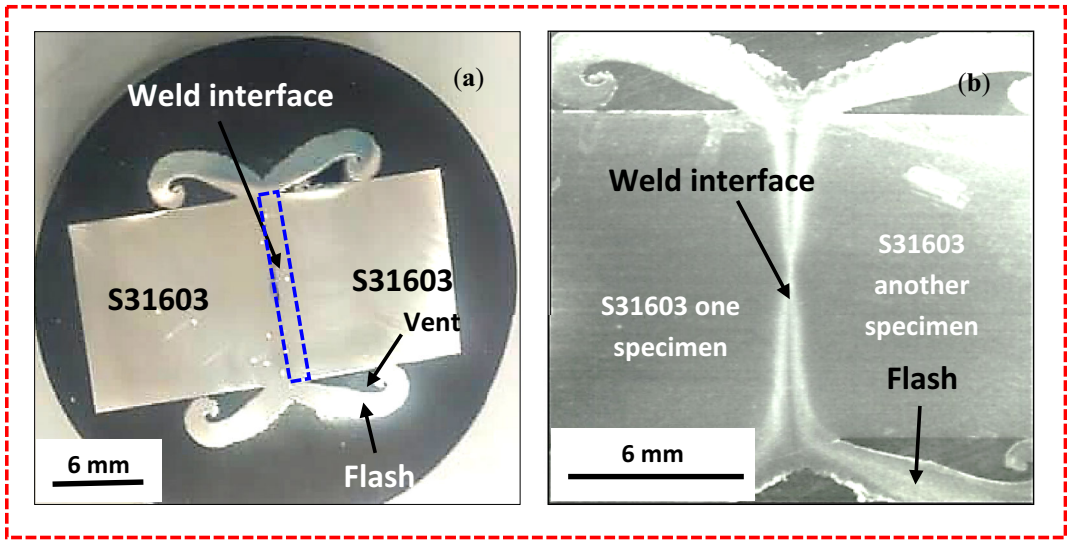

Figure 3. (**a**) weld specimen and (**b**) macrostructure of A4 steel (UNS S31603) similar joint.

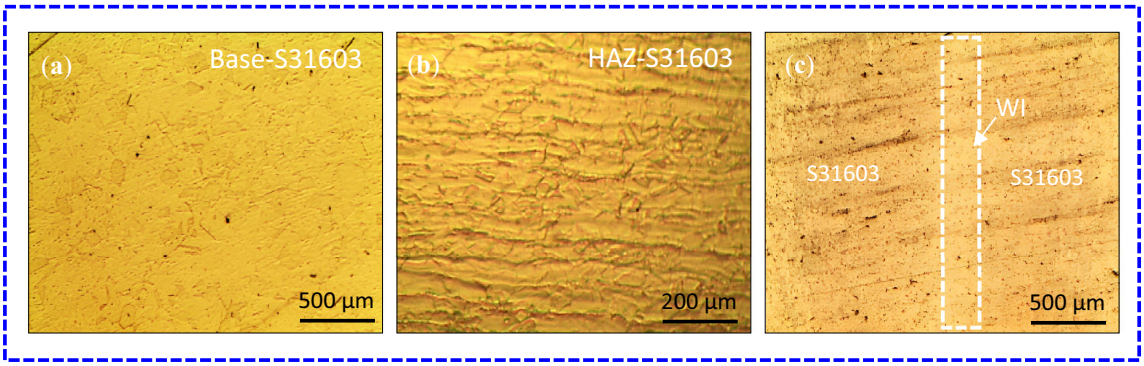

Figure 4. Optical microstructure (**a**) base of UNS S31603, (**b**) HAZ of UNS S31603 joint and (**c**) weld interface of UNS S31603 joint.

strength and reduces the ductility and elastic elongation due to the residual stresses, and limited ability of fine grains to deform elastically. Excessive heat input or incorrect parameters might potentially diminish ductility within the heat-affected zone (HAZ). Proper control of welding parameters is essential to maintain the desired microstructure and ensure optimal mechanical performance. Figure 6(e) illustrates the calculated joint efficiency (η) for the friction welding process under study. Surprisingly, the efficiency was determined to be 147%. This result exceeding 100% indicates that the strength of the weld joint surpassed that of the parent metal. This study showcased exceptional outcomes in the joining of A4 stainless steel, evident through the joint efficiency surpassing 100%. Joint efficiency serves as a measure of how effectively a welded joint can transmit applied loads compared to the base material. When the weld quality is high, and the weld material's strength matches that of the base material, the joint efficiency would typically be 100%.

3.4 *Microhardness of weldment*

It is crucial to recognize that microhardness values can fluctuate within various areas of the welded joint. Microhardness analysis in the weld zone, parent metal (PM), and heat-affected zone (HAZ) regions was carried out using a Vickers tester. This involved preparing cross-sectional samples from the welded region. Microhardness measurements are typically obtained by assessing the specimen's resistance to indentation under a specific load (0.01 kg) for a dwell time of 10 seconds. In this study, the test was conducted for three trials to ensure accurate and consistent results. The results obtained are presented in figure 7(a). The graph illustrates that the microhardness values in the weld zone region are higher compared to the HAZ and parent metal. The values gradually decreased from the weld zone (257 Hv0.01) towards the parent metal (246 Hv0.01), as indicated by the arrow movement in figure 7(b). A4 steel generally possesses relatively high hardness owing to its

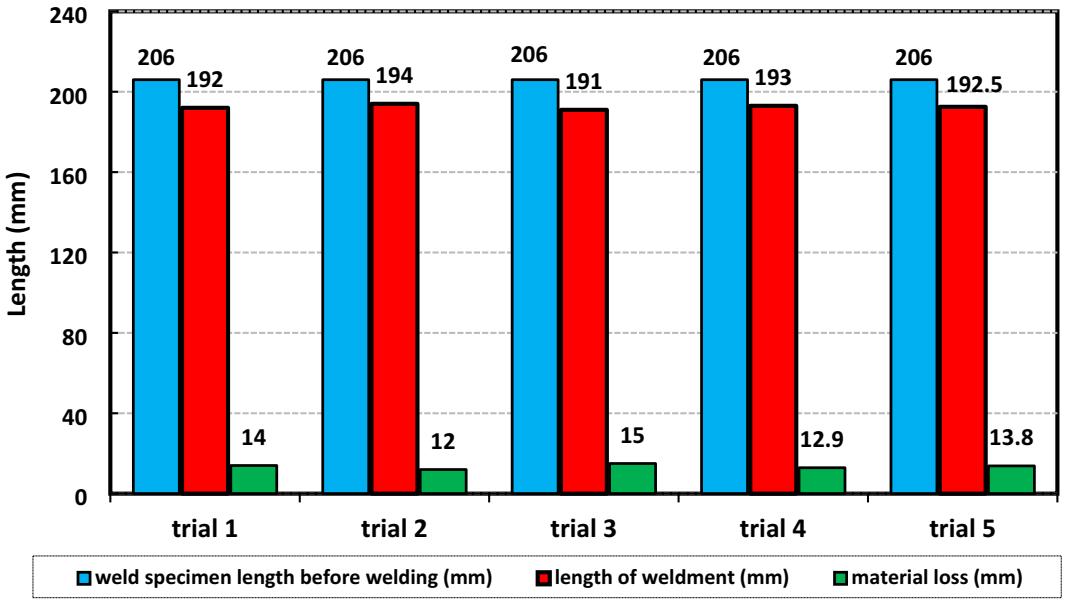

Figure 5. Axial shortening results observed compared to weldments.

composition. However, during the FW process, the developed temperature and pressure applied over time can potentially influence the microhardness of the joint near the weld zone. In most cases, the heat generated at the interfaces of faying surfaces during friction welding can lead to grain refinement or the formation of new phases within the microstructure. During FW, the intense heat and pressure applied to the faying surfaces result in dynamic recrystallization within the weld zone. This process leads to the formation of a refined and more uniform microstructure with smaller grain sizes compared to the coarse grain structure typically found in the HAZ. The presence of finer grains in the weld zone contributes to higher hardness. Finer grains offer more grain boundaries, which act as barriers to dislocation movement and contribute to increased hardness by impeding plastic deformation. While HAZ experiences significant temperature gradients when moving away from the weld interface towards the unaffected base material. This thermal gradient results in variations in cooling rates across the HAZ. Additionally, the heat input from the welding process causes the HAZ to reach temperatures close to or within the range of its recrystallization temperature. At these elevated temperatures, the existing grains in the HAZ may grow larger as a result of grain coarsening. This phenomenon may affect the hardness in the HAZ, causing it to be comparatively lower than the weld. Specifically, the parent metal zone exhibits a hardness of approximately 246 HV0.01, while in the Heat-Affected Zone (HAZ) region, the hardness measures 252 HV0.01. Consequently, the HAZ region demonstrates superior hardness compared to the parent zone and is inferior to the weld zone, which had 257 HV0.01. Here, the weld joint is better since the increased hardness values imply a potential susceptibility to strength in the welded joint compared to the base metal [21]. Further, the optimization of mechanical properties will necessitate post-welding heat treatment. As illustrated in figures 4(b)-(c), the heat generated during AISI316L FW may lead to the transformation of austenitic grains with grain refinement and potential sensitization. The formation of a softer phase (ferrite), can contribute to a decrease in hardness in the base metal. In friction welding, the hardness can be influenced by factors such as the welding parameters, cooling rate, and metallurgical changes occurring during the welding process. Finally, an increase in hardness indicates improved strength and wear resistance, but excessive hardness can lead to reduced toughness.

3.5 *Impact and bending testing of fabricated welds*

Specimens, prepared according to the ASTM E23 standard from the welded samples, were subjected to the Charpy V-notch test. Different regions, namely the weld, Heat-Affected Zone (HAZ), and Parent Metal (PM), were analyzed, and the results are presented in figure 8(a). The Charpy test was employed to assess the impact toughness of the joint. The results revealed that the performance of the weld zone was relatively poor when compared to the PM and HAZ. Though the FW produced a strong metallurgical bond between the faying surfaces without the need for additional filler material, it reduced ductility, particularly at the weld interface. It might introduce discontinuities and variations in the microstructure that affect the material's toughness. This discrepancy was attributed to the weld

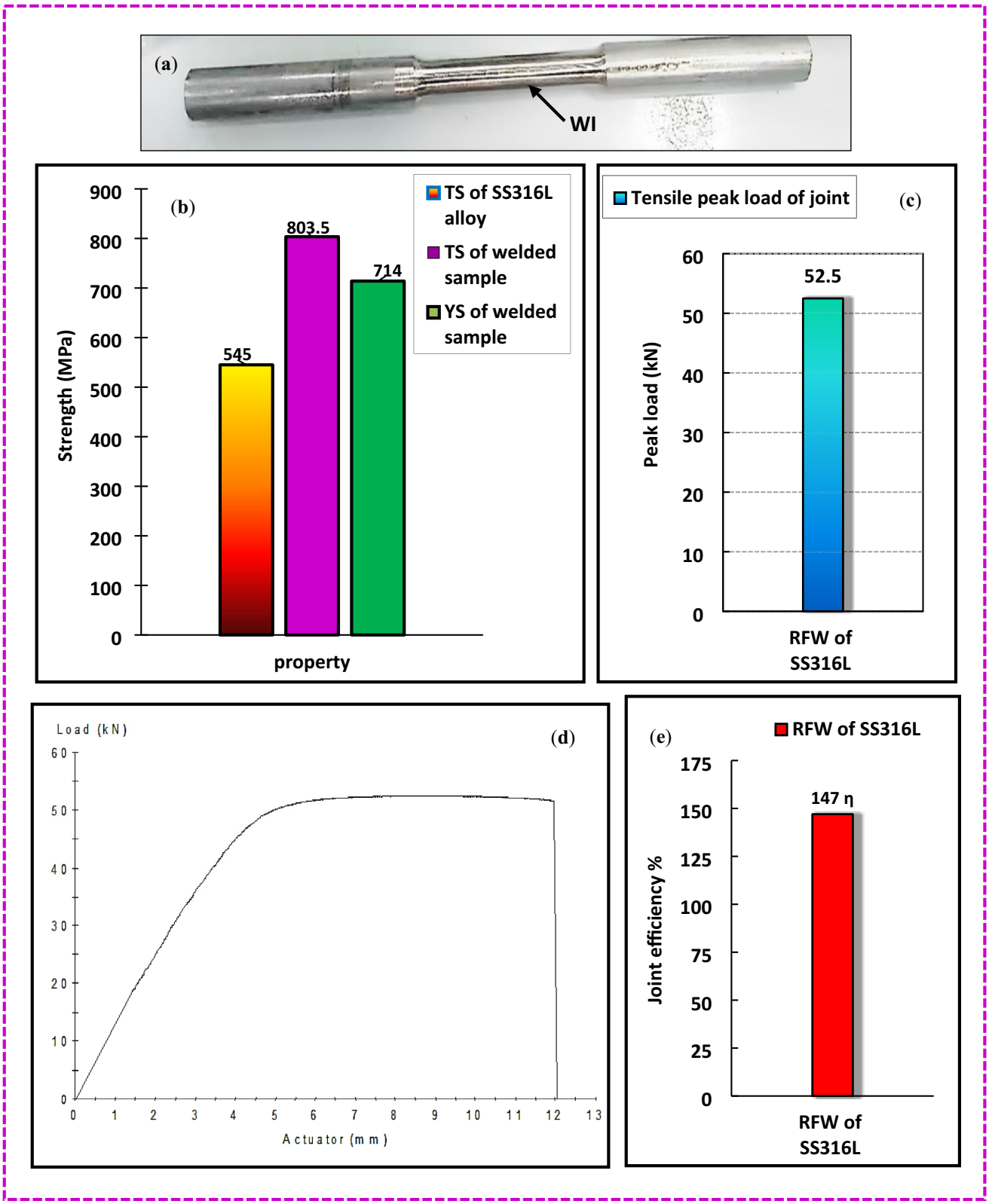

Figure 6. (**a**) weld specimen prepared for tensile testing, (**b**) tensile (TS) and yield strength (YS) of SS316L alloy and weld, (**c**) peak load value obtained for the weld, (**d**) load vs deflection curve of tensile testing and (**e**) joint efficiency of this study.

zone's plastic nature post-welding. The samples fractured, yielding average values of 26 J and 90 J in the weld and HAZ regions, respectively. These values were significantly lower compared to the PM (162 J) since friction welding involved localized heating and open cooling, leading to varying impact toughness across different regions. In most metals, the hardness and impact strength are inversely proportional to each other. The fine grains at the weld zone exhibited high hardness, suggesting a low impact resistance since it has less energy-absorbing capability compared to coarser-grained structures which could contribute to the reduced impact strength. This can lead to increased susceptibility to brittle fracture upon impact loading and reduced ability to deform plastically under impact loading. Stress concentration at grain boundaries, particularly in regions of high strain can lead to localized weakening and facilitate crack initiation and propagation (fine grain boundaries in weld zones are inherently weaker regions and have a higher volume fraction) under impact loading conditions. Consequently, intergranular fracture happens in the weld with a low toughness value as it is more susceptible to impact fracture. The formation of grain boundary embrittlement can lead to reduced impact toughness in the weld zone. To enhance toughness, it is recommended to minimize post-weld residual stresses. At last, factors like enhanced stress concentration, limited ductility, grain sizes, grain boundary fracture, and lack of microstructural homogeneity can make poor toughness in the welds.

The bending test was conducted on the sample following the ASTM E290 standard. Figure 8(b) represents the load (y-axis) and displacement (x-axis) curve obtained during the bending test. This graph illustrates the behaviour of the weld specimen under the bending test conditions. The bending test serves as a valuable tool to assess the strength and flexibility of the A4 friction-welded joint. The weld sample exhibited elasticity until a 2 mm deflection, after which it displayed plastic behaviour. Between 3 mm and 15 mm of actuation, the curve depicting the applied load gradually increased, reaching a maximum of 19 kN (figure 8(c)) without any signs of bending in the weldment. The applied load was incrementally raised until it reached the specified displacement. Upon surpassing this point, the weld failed the bending test, leading to a sudden drop in the load at a particular actuation. During the testing process, this load induced tensile stress on one side of the sample and compressive stress on the other side. Bending tests hold paramount importance across various industries, including automotive, aerospace, construction, and manufacturing. They play a crucial role in the control and design of components that necessitate flexibility or resistance against bending forces.

4. Conclusions

The successful frictional joining of A4 stainless steel at room temperature, utilizing low friction pressure and brief friction time, marked a significant advancement. A meticulous analysis of the welded specimens was carried out to comprehend their behaviour based on the selected process parameters. Macrographs showcased flawless weld zones, devoid of any scars or defects. Achieving an exceptionally narrow weld interface (WI) and retaining an excellent surface finish even after machining was noteworthy. The expelled flash, during welding, exhibited uniformity on both sides, coiling uniformly. Remarkably, under these specific parameters, a formidable weld strength of 803 MPa

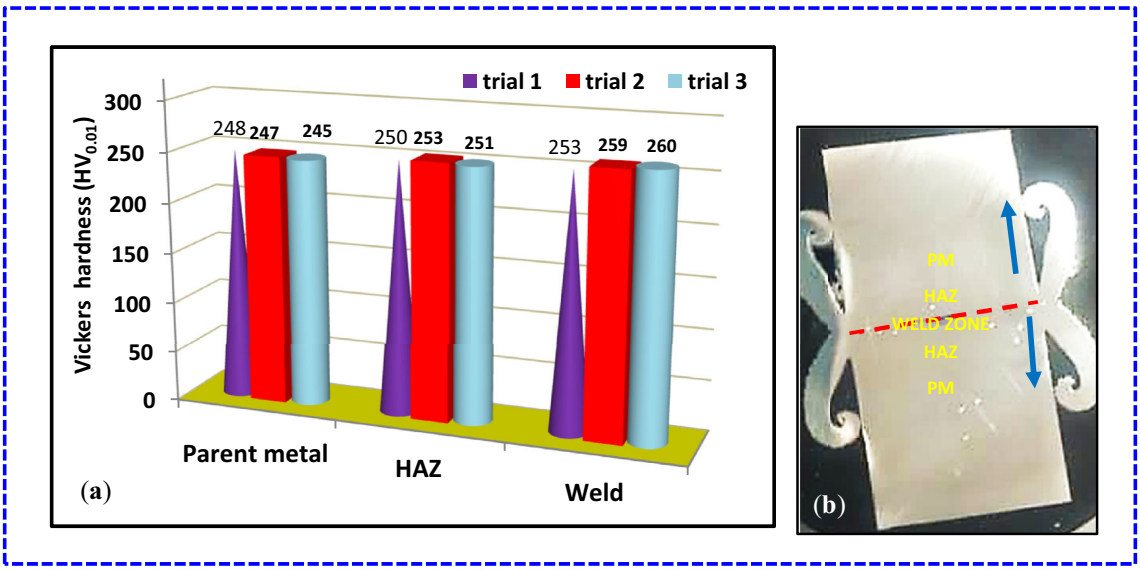

Figure 7. (**a**) Vickers microhardness measurements and (**b**) different zones in similar welded samples for hardness measurement.

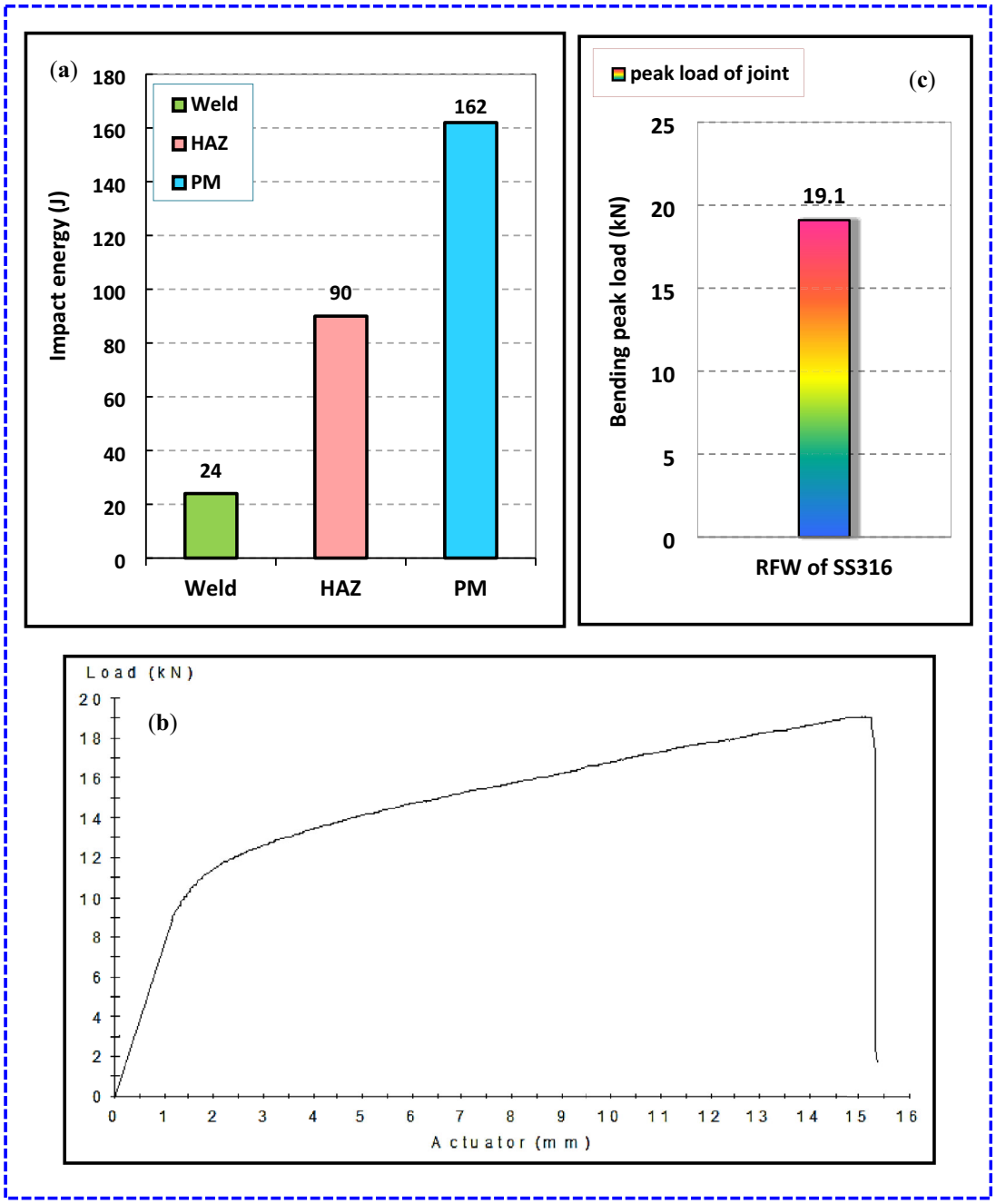

Figure 8. (**a**) Charpy test results, (**b**) bending-load vs. deflection and (**c**) peak load during bending.

was attained, resulting in an impressive 147% joint efficiency. This accomplishment holds immense significance, indicating our ability to produce high-quality welds with superior strength compared to the base material (PM). However, weld tests indicated relatively lower values for hardness (10 Hv0.01) and impact toughness (approximately 70 J) in the weld zone compared to the Heat Affected Zone (HAZ). This disparity was attributed to the formation of an equiaxed homogeneous structure in the weld zone, which diminished microhardness and impact toughness due to its plastic nature. In bending tests, the samples exhibited elasticity until a 2 mm deflection and reached their peak load at 19 kN, underscoring their structural integrity and resilience under applied stress.

Funding No funding was obtained for this study.

Declarations

Conflict of interest The authors declare that there is no conflict of interest.

References

[1] Bhamji I, Preuss M, Threadgill P L, Moat R J, Addison A C and Peel M J 2010 Linear friction welding of AISI 316L stainless steel, *Materials Science and Engineering: A*. 528 (2): 680–690. https://doi.org/10.1016/j.msea.2010.09.043

[2] Kotecki Damian and Frank Armao 2003 Stainless Steels Properties – How To Weld Them Where To Use Them, *Lincoln Electric*. C64000:1-37

[3] Rajak Dipen Kumar, Pagar Durgesh D, Pradeep L. Menezes and Eyvazian Arameh 2020 Friction-based welding processes: friction welding and friction stir welding. *Journal of Adhesion Science and Technology*. 34(24): 2613–2637. https://doi.org/10.1080/01694243.2020.1780716

[4] Ahmadi E and Ebrahimi A R 2015 Welding of 316L Austenitic Stainless Steel with Activated Tungsten Inert Gas Process. *Journal of Mater. Eng. and Perform.* 24: 1065–1071. https://doi.org/10.1007/s11665-014-1336-6

[5] Subramanian S M, Paulraj S and Abdul Haq N H 2021 Effect of faying surfaces and characterization of aluminium AA6063–steel AISI304L dissimilar joints fabricated by friction welding with hemispherical bowl and threaded faying surfaces. *Int. J. Adv. Manuf. Technol.* 116: 629–666. https://doi.org/10.1007/s00170-021-07445-0

[6] Murugan Senthil S, Sathiya P and Haq A N 2021 Continuous drive dissimilar friction welding of wrought aluminium 6063–T6 and austenitic stainless steel 304L with different faying surfaces and welding trials. *Kovové Materiály - Metallic Materials*. 59(3): 161–179. https://doi.org/10.4149/km_2021_3_161

[7] Murugan Senthil S, Sathiya P and Haq A N 2020 Experimental study on the effect of silver, nickel and chromium interlayers and upset pressure in joining SS304L-AA6063 alloys through direct drive friction welding process. *J. Braz. Soc. Mech. Sci. Eng.* 42: A.No. 611. https://doi.org/10.1007/s40430-020-02687-7

[8] Murugan Senthil S, Sathiya P and Haq A N 2020 Effect of welding parameters on the microstructure and mechanical properties of the friction-welded dissimilar joints of AA6063 alloy and faying surface-tapered AISI304L alloy. *Welding in the World*. 64: 483–499. https://doi.org/10.1007/s40194-020-00846-x

[9] Wan L and Huang Y 2018 Friction welding of AA6061 to AISI 316L steel: characteristic analysis and novel design equipment. *Int. J. Adv. Manuf. Technol.* 95: 4117–4128. https://doi.org/10.1007/s00170-017-1505-5

[10] Li P, Dong H, Xia Y, Hao X, Wang S, Pan L and Zhou J 2018 Inhomogeneous interface structure and mechanical properties of rotary friction welded TC4 titanium alloy/316L stainless steel joints. *Journal of Manufacturing Processes* 33: 54–63. https://doi.org/10.1016/j.jmapro.2018.05.001

[11] Khidhir G I and Baban S A 2019 Efficiency of dissimilar friction welded 1045 medium carbon steel and 316L austenitic stainless steel joints. *Journal of Materials Research and Technology* 8(2): 1926–1932. https://doi.org/10.1016/j.jmrt.2019.01.010

[12] Mishra Neeraj Kumar and Shrivastava Amber 2023 Improvement in strength and ductility of rotary friction welded Inconel 600 and stainless steel 316L with Cu interlayer. *CIRP Journal of Manufacturing Science and Technology*. 41: 19–29. https://doi.org/10.1016/j.cirpj.2022.12.006

[13] Çetkin E, İmak A and Kirik I 2023 Investigation Microstructure and Mechanical Properties of Ramor and Stainless Steel Joined by Friction Welding. *J. Mater. Eng. and Perform.* 32: 2522–2533. https://doi.org/10.1007/s11665-022-07625-3

[14] Astarita Antonello, Scherillo Fabio, Curioni Michele, Aprea Paolo, Impero Filomena, Squillace Antonino and Zhou Xiaorong 2016 Study of the Linear Friction Welding Process of Dissimilar Ti-6Al-4V–Stainless Steel Joints. *Materials and Manufacturing Processes*. 31(16): 2115–2122. https://doi.org/10.1080/10426914.2016.1151048

[15] Arivazhagan N, Surendra Singh, Satya Prakash and Reddy G M 2011 Investigation on AISI 304 austenitic stainless steel to AISI 4140 low alloy steel dissimilar joints by gas tungsten arc, electron beam and friction welding. *Materials & Design* 32(5): 3036–3050. https://doi.org/10.1016/j.matdes.2011.01.037

[16] Çavuşoğlu N 2022 Effect of Friction Welding Parameters on the Mechanical and Microstructural Properties of Dissimilar IN713C-AISI 4140 Joints. *J. Mater. Eng. and Perform.* 31: 4035–4048. https://doi.org/10.1007/s11665-021-06474-w

[17] Dahlan, Hendery, Ahmad Kafrawi Nasution, Sulthan Asyraf Zuhdi and Meifal Rusli 2023 Study of the Effect of Friction Time and Preheating on the Joint Mechanical Properties of Friction Welded SS 316-Pure Zn. *Applied Sciences* 13(2): 988. https://doi.org/10.3390/app13020988

[18] Jignesh Patel, Bimal Kumar Mawandiya, Kaushik Patel, Mayur A Makhesana, Manish Gupta, Karrar Hazim Salem and Satbir S Sehgal 2023 Experimental investigations and effect of parameters on friction welded AISI 304 and Invar alloys. *Advances in Materials and Processing Technologies*. https://doi.org/10.1080/2374068X.2023.2233855

[19] Liu Huihong and Fujii Hidetoshi, 2021 Ultralow rotation speed produces high-quality joint in dissimilar friction welding of Ti–6Al–4V alloy and SUS316L stainless steel, *Materials Science and Engineering: A*, 800: A.No.140303. https://doi.org/10.1016/j.msea.2020.140303

[20] Karabey Ome and Akkus Ahmet 2022, Effect of Welding Parameters on Axial Shortening in Continuous Friction Welded Inconel 718 Superalloy and AISI 316L Stainless Steel, *European Journal of Science and Technology*, 34: 311-316. https://doi.org/10.31590/ejosat.1081747

[21] Talabi S I, Owolabi O B, Adebisi J A and Yahaya T 2014, Effect of welding variables on mechanical properties of low carbon steel welded joint, *Advances in Production Engineering and Management*, 9(4):181-186. https://doi.org/10.14743/apem2014.4.186